

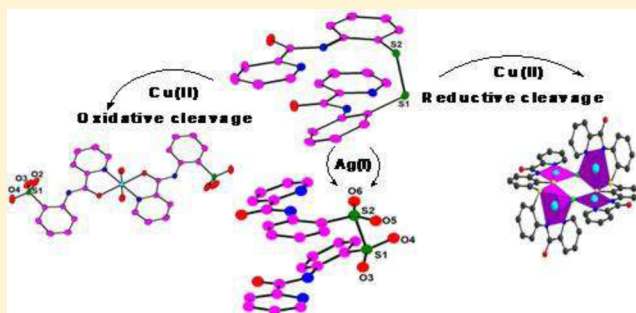
Copper(II)-Catalyzed Disulfide Scission—Stepwise Aerobic Oxidative Cleavage to Sulfinate and Sulfonate and Reductive Anaerobic Cleavage to Thiols

Isha Lumb, Maninder Singh Hundal,* and Geeta Hundal*

Department of Chemistry, Centre for Advanced Studies in Chemistry, Guru Nanak Dev University, Amritsar-143005, India

S Supporting Information

ABSTRACT: The Cu(II)-catalyzed oxidative and reductive cleavage of the disulfide bond of *N*-(2-(2-(2-picolinamido)phenyl)disulfanyl)phenyl)picolinamide, **L**, is reported for the first time. Aerobic oxidation with Cu(II) gives complete oxidation of S–S bond to sulfonates, whereas Ag(I) gives only partial oxidation up to sulfinate, in the absence of any other oxidizing agent, in tetrahydrofuran/water solution. The *in situ* generated sulfonate product forms a thermally stable, two-dimensional H-bonded polymeric complex with Cu(II) ions in two polymorphic forms. **L** in the presence of Cu(II), in an inert atmosphere, results in a reductive cleavage of the disulfide bond and an *in situ* formation of a new C–S bond. The latter forms a unique tetranuclear complex with Cu(II) employing deprotonated amide groups and bridging thiol and chloride atoms. The disulfide precursor and the products were characterized by X-ray crystallography and spectroscopic techniques.



INTRODUCTION

The disulfide bond plays an important role in the structure, folding, and stability of the proteins as it is the only readily reversible covalent cross-linking bond present in native proteins.¹ Thus, formation and cleavage of disulfide bonds is known to be important for biological activity of several S-containing proteins.² The thiol–disulfide systems show a rich redox chemistry³ that involves oxidation of thiols to disulfides⁴ or to sulfenates/sulfonates/sulfonates;⁵ reductive cleavage of disulfides to thiols,⁶ occasionally followed by C–S or C–N cleavage;⁷ oxidation of disulfide, with S–S preservation to form any or a mixture of sulfenates/thiosulfenates/sulfonates/thiosulfonates;⁸ or total oxidative cleavage to sulfonates.⁹ The oxidation of thiols to disulfides can be achieved in a variety of ways by using transition metals, metal oxides, hydrogen peroxides, oxygen,¹⁰ or autoxidation.¹¹ Commonly the peracids are used¹² to oxidize organo disulfides, but hydrogen peroxide in acetic acid has also been used. However, the latter, in the absence of a catalyst (molybdates and tungstates, methyltrioxorhenium(VII))¹³ warrants harsh conditions.¹⁴ The role of transition metal ions in the disulfide chemistry, however, is very versatile and interesting especially in the case of copper, which itself has a good redox chemistry. When the facile oxidation of 2,2'-dipyridyl disulfide (2-pydi) to pyridine-2-sulfinate in the presence of the Cu(II) ion and water under both aerobic/anaerobic conditions was reported,¹⁵ it was believed that further oxidation of disulfides or sulfinate compounds to the corresponding sulfonates would require a strong oxidizing agent such as hydrogen peroxide or halogen. This was negated by the unexpected, complete oxidation of 3-methyl-2-pydi to its

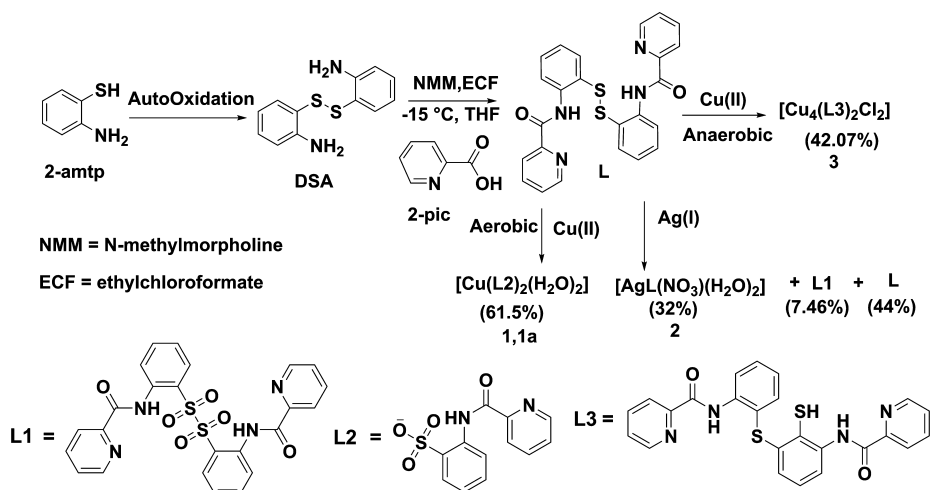
sulfonate (in low yield)¹⁶ and later of 2-pydi to its sulfinate/sulfonate mixture,¹⁷ in the presence of Cu(II) ion, without any other oxidizing agent in very mild conditions. Such an oxidation phenomenon is akin to oxidative desulfurization and the metabolism of sulfur *in vivo*.¹⁸ A similar case was later reported for 4,4'-dipyridyldisulfide (4-pydi), which also gave direct oxidation¹⁹ to sulfonate in the presence of Cu(II), albeit in coexistence with the disulfide in some cases.

In our pursuit of studying amide-based complexes²⁰ and searching for new coordination complexes with *in situ*-formed ligands, not easily accessible otherwise, we here present *N*-(2-(2-(2-picolinamido)phenyl)disulfanyl)phenyl)picolinamide **L** (Scheme 1). The reactions of **L** with Ag(I) and Cu(II), in aerobic conditions, reveal the respective formations of sulfinate **L1** and sulfonate **L2** indicating that these metal ions help in oxidation of the S–S bond. The sulfonate **L2** forms a thermally stable, two-dimensional (2D) H-bonded supramolecular complex with copper. **L**, **L1**, and the copper(II) complex of **L2** were characterized with X-ray diffraction (Supporting Information, Table S1). The oxidation of **L**, in the case of Cu(II), is complete forming two polymorphs (**1**) and (**1a**) of a copper(II) complex of **L2**, whereas Ag(I) gives a mixture of **L**, **L1**, and an uncharacterized complex of Ag(I). We also give X-ray structural evidence for the new tetranuclear complex [Cu₄(**L3**)₂Cl₂] formed as a result of the reductive cleavage of disulfide bond concomitant with *in situ* formation of a new C–S bond, in the presence of Cu(II), under anaerobic conditions.

Received: May 16, 2014

Published: June 30, 2014

Scheme 1



Interestingly the ligand **L** was first prepared by a different method⁶ by Tyler et al.,^{6a} cleaved reductively (using NaBH_4) to its corresponding thiol, and then its Co(III) complexes were oxidized by H_2O_2 to give sulfonates of the bound thiol. The same ligand, in its anionic form, was also used by Wang et al.^{6b} to study reductive cleavage of the disulfide bond by V(IV). However, neither **L** was structurally characterized in any of these two reports nor was its oxidative cleavage studied in the presence of Ag(I) and Cu(II) ions. This is also the first time that a reductive cleavage of the disulfide bond has been found for this by just using Cu(II) ions only.

EXPERIMENTAL DETAILS

Materials and Methods. The solvents were distilled prior to use following appropriate procedures.²¹ Under the N_2 atmosphere dry methanol is used as solvent. All the chemicals were purchased from Aldrich and used as received. Elemental analyses (C, H, N, S) were performed on a Perkin–Elmer model 2400 CHN analyzer. IR spectra were recorded as KBr pellets on a Varian 660-IR FT-IR spectrophotometer. Thermal analyses were carried out on a SII 6300 EXSTAR TG/DTA thermo analyzer in flow of N_2 , in the temperature range from 20 to 800 °C, with a heating rate of 10 °C min^{-1} . The ^1H NMR spectra were recorded on a 300 MHz JEOL FT NMR spectrometer with tetramethylsilane as the reference compound in CDCl_3 , deuterated dimethyl sulfoxide ($\text{DMSO}-d_6$), or trifluoroacetic acid (TFA) as per needs. UV–vis spectra were recorded on a Shimadzu Pharmaspec UV-1700 UV–vis spectrophotometer. The powder X-ray diffraction (PXRD) was carried out on Rigaku miniflex 2 in the range of $\theta = 2^\circ$ to 60° . Cyclic voltammetric (CV) measurements were carried out on a BAS CV 50W electrochemical analyzing system (accuracy 1.0 mV). The CVs of (**1**) and (**3**) were recorded in DMSO (dimethyl sulfoxide) with 0.1 M TBAP (tetrabutylammonium perchlorate) as supporting electrolyte using a three-electrode system under N_2 atmosphere. CVs of complexes **1** and **3** displaying $\text{Cu}^{2+}/\text{Cu}^+$ (E_1) and Cu^+/Cu^0 (E_2) couples in DMSO at Pt working electrode; Pt wire as the counter electrode; and Ag/Ag^+ as the reference electrode. The potentials were corrected and reported versus saturated calomel electrode (SCE), standardized for the redox couple ferricinium/ferrocene. High-resolution mass spectra (HRMS) were recorded on a Bruker microTOF-QII spectrophotometer. Magnetic moment was carried out on a Johnson Matthey Catalytic Systems Division Equipment, at room temperature, using the molecular weight for the tetramer complex (**3**).

Caution! Perchlorate salts are explosive in nature. It could explode upon heating and should be handled in small amounts with caution.

EXPERIMENTAL SECTION

(1). Synthesis of 2-(2-(2-(2-aminophenyl)disulfanyl)benzenamine). The 2-aminothiophenol (2-amtp) (3 g) was dissolved in 25 mL of acetonitrile and was oxidized in air. Upon slow evaporation, the crystals of 2-(2-(2-aminophenyl)disulfanyl)benzenamine (DSA) were grown after a few days. Yield: 2.7 g (90%). ^1H NMR [300 MHz; CDCl_3]: δ (ppm) 6.5 (d, 2H, ArH, $J = 1.2$ Hz), 6.7 (d, 2H, ArH, $J = 1.2$ Hz), 7.13 (t, 2H, ArH, $J = 1.5$ Hz), 7.17 (t, 2H, ArH, $J = 1.5$ Hz), 4.3 (s, 1H, NH).

(2). Synthesis of N-(2-(2-(2-(2-picolinamido)phenyl)disulfanyl)phenyl)picolinamide, L. This ligand was prepared by mix anhydride coupling reaction,²² which is an easy and convenient approach. To the stirred solution of 0.734 g (5.9 mmol) of picolinic acid (2-pic) in dry THF at -15°C , N-methyl morpholine (NMM) (0.213 mL, 1.93 mmol) and ethylchloroformate (ECF) (0.213 mL, 2.2 mmol) were added. After 20 min of stirring, 2-(2-(2-aminophenyl)disulfanyl)benzenamine (DSA) (0.37 g, 1.49 mmol) was added (in dry THF), and the reaction mixture was stirred for 2 h at -15°C . The stirring was later continued at room temperature for an additional 10 h. The reaction was monitored by using thin-layer chromatography (TLC). On completion, the reaction mixture was concentrated to remove the THF and then extracted into ethyl acetate. The organic layer was dried over sodium sulfate and was concentrated under vacuum, to get crude creamish solid, which was recrystallized from chloroform/acetonitrile to get diffraction-quality crystals. Yield 0.60g (88%). mp 170–173 °C. Anal. Calc. for $\text{C}_{24}\text{H}_{18}\text{N}_4\text{O}_2$ S₂: C, 62.48; H, 3.93; N, 12.22; S, 13.87. Found: C, 62.33; H, 3.99; N, 12.14; S, 13.59%. m/z : 459.09 [$\text{M} + 1$]⁺, (calculated 459.09). IR (KBr/ cm^{-1}) 3272, 3060, 1699, 1572, 1428, 1299. ^1H NMR [300 MHz; CDCl_3 , Me_4Si] δ (ppm) 6.89 (t, 2H, ArH, $J = 7.5$ Hz), 7.21 (t, 2H, ArH, $J = 7.5$ Hz), 7.4 (d, 2H, ArH, $J = 7.8$ Hz), 7.48 (d, 2H, ArH, $J = 7.5$ Hz), 7.88 (t, 2H, PyH, $J = 7.8$ Hz), 8.24 (d, 2H, PyH, $J = 7.8$ Hz), 8.45 (d, 2H, PyH, $J = 8.7$ Hz), 8.56 (d, 2H, PyH, $J = 7.5$ Hz), 11.01 (s, 1H, NH). ^{13}C NMR [75 MHz; CDCl_3] δ 120, 122, 123, 124, 126, 131, 136, 137, 139, 148, 149, 161.9.

(3). Synthesis of $[\text{Cu}(\text{L}2)_2(\text{H}_2\text{O})_2] \cdot \text{H}_2\text{O}$ (1). Copper(II) chloride dihydrate (0.170 g, 1 mmol) in water and **L** (0.458 g, 1 mmol) in THF were mixed with continuous stirring for 1 h. There was an immediate color change from yellow to dark green. After stirring for 1 h, the solution was filtered. Green crystals of (**1**) separated out from the filtrate after several days. Yield: 0.40 g (61.5%). mp > 300 °C. Anal. Calc. for $\text{C}_{24}\text{H}_{24}\text{CuN}_4\text{O}_{11}\text{S}_2$: C, 42.80; H, 3.57; N, 7.90; S, 9.50. Found: C, 42.43; H, 3.42; N, 7.45; S, 9.39%. m/z : 656.89 [$\text{M} + 2$]⁺ (calculated 656.13). UV–vis [λ_{max} (DMSO)/nm (ϵ , $\text{M}^{-1}\text{cm}^{-1}$): 697 (57.4), 290 (23540)]. IR (KBr/ cm^{-1}) 3428, 3029, 1631, 1586, 1444, 1359, 1219, 1015. μ_{eff} (B.M.): 1.98.

(4). Synthesis of Bis-N-(2-(sulfonyl)phenyl)picolinamide, L1. The ligand **L** was dissolved in THF and added into a solution of AgNO_3 in methanol. White precipitates, separated from the reaction

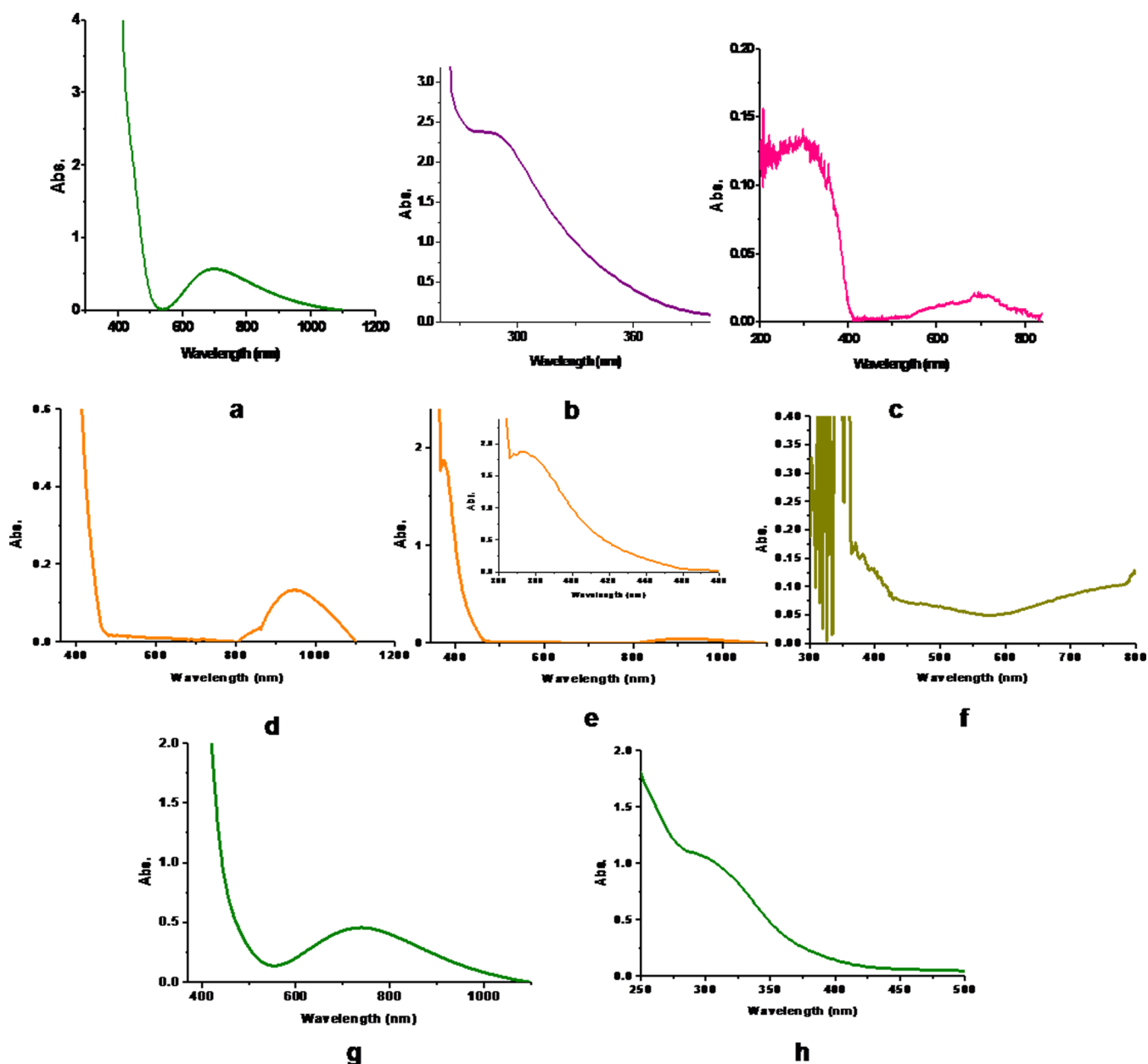


Figure 1. UV-vis spectra of complex (1) in DMSO showing (a) d-d bands, (b) CT band, and (c) diffuse reflectance spectra. The UV-vis spectra of complex (3) (d) in DMSO, showing d-d bands (e) in DMSO, showing CT band, inset- expanded CT region (f) d-d band in the diffuse reflectance spectra (g) showing d-d bands in methanol (h) CT band in methanol.

mixture after 15 min, were filtered out. The TLC of filtrate showed that it contained both L and L1. To separate them, the filtrate was evaporated and treated with CHCl_3 to extract L, while L1 was left as a solid product soluble in DMSO only. (% yields of L and L1 = 44 and 7.46, respectively). The crystals of L1 were obtained by vapor diffusion method using DMSO/diisopropyl ether. Light yellowish crystals were obtained after a month. Yield: 0.4 g (7.46%). mp 272–275 °C. Anal. Calc. for $\text{C}_{24}\text{H}_{18}\text{N}_4\text{O}_6\text{S}_2$: C, 55.16; H, 3.59; N, 10.72; S, 12.77. Found: C, 54.96; H, 3.80; N, 10.80; S, 13.01%. m/z : 523.07 [$\text{M} + 1$]⁺ (calculated 523.07). IR ($\text{KBr}/\text{cm}^{-1}$) 3438, 3096, 1696, 1588, 1300, 1440, 1215, 1012. ^1H NMR [300 MHz; DMSO- d_6 ; Me $_4$ Si] δ (ppm) 7.08 (t, 2H, ArH, $J = 9$ Hz), 7.36 (t, 2H, ArH, $J = 9$ Hz), 7.63 (t, 2H, ArH, $J = 8.4$ Hz), 7.74 (d, 2H, ArH, $J = 9$ Hz), 8.03 (t, 2H, PyH, $J = 9$ Hz), 8.16 (d, 2H, PyH, $J = 8.1$ Hz), 8.49 (d, 2H, PyH, $J = 7.2$ Hz), 8.7 (s, 2H, PyH), 11.9 (s, 1H, NH).

(5). Synthesis of $[\text{AgL}(\text{NO}_3)(\text{H}_2\text{O})_2]$ (2). The complex (2) separated as a white precipitate (*vide supra*), and it is insoluble in all solvents. This precipitate was washed with chloroform to remove any

untreated ligand and dried under vacuum. Yield: 0.28 g (32%). mp > 290 °C. Anal. Calc. for $\text{C}_{24}\text{H}_{22}\text{AgN}_3\text{O}_7\text{S}_2$: C, 43.38; H, 3.34; N, 10.54; S, 9.65. Found: C, 43.23; H, 3.23; N, 10.14; S, 9.50%. m/z : 663.43 [$\text{M} - 1$]⁺ (calculated 663.46). IR ($\text{KBr}/\text{cm}^{-1}$) 3436, 3270, 1691, 1523, 1430, 1309. ^1H NMR [300 MHz; TFA + CDCl_3 ; Me $_4$ Si] δ (ppm) 7.3 (t, 2H, ArH, $J = 8.4$ Hz), 7.46 (t, 2H, ArH, $J = 7.8$ Hz), 7.57 (d, 2H, ArH, $J = 7.8$ Hz), 7.72 (d, 2H, ArH, $J = 7.8$ Hz), 8.32 (t, 2H, PyH, $J = 6.6$ Hz), 8.6 (d, 2H, PyH, $J = 8.1$ Hz), 8.82 (d, 2H, PyH, $J = 8.1$ Hz), 9.96 (s, 2H, PyH, $J = 6.6$ Hz), 11.9 (s, 1H, NH).

(6). Synthesis of Complex $[(\text{Cu})_2(\text{L3})\text{Cl}]_2$ (3). This complex was prepared from a reaction mixture containing equimolar amounts of Cu(II) chloride dihydrate (0.170 g, 1 mmol) and ligand L (0.458 g, 1 mmol) dissolved in a minimal amount of acetonitrile under N_2 atmosphere. A green colored solid separated out, which was filtered and dried *in vacuo*. The solid obtained was redissolved in lukewarm methanol and kept in an airtight container. Small blackish-green colored crystals appeared in the solution after about a month, which were suitable for the X-ray diffraction studies. Yield: 0.52 g (42.07%).

mp > 290 °C. Anal. Calc. for $C_{24}H_{15}Cu_2ClN_4O_2S_2$: C, 46.64; H, 2.42; N, 9.06, S, 10.38. Found: C, 46.30; H, 2.12; N, 8.77; S, 10.51%. m/z : 618.80 $[M]^+$ (calculated 618.05). UV-vis $[\lambda_{max}(\text{CH}_3\text{OH})/\text{nm} (\epsilon, \text{M}^{-1} \text{cm}^{-1})]$: 736 (47.6) and 302 (10570), $[\lambda_{max}(\text{DMSO})/\text{nm} (\epsilon, \text{M}^{-1} \text{cm}^{-1})]$: 911 (48), 374 (1874). IR (KBr/ cm^{-1}): 3435, 3055, 1596, 1475, 1304. μ_{eff} (B.M.): 3.17.

X-ray Data Collection. The data for **L**, **L1**, **(1)**, **(1a)**, and **(3)** were collected on a Bruker Apex-II CCD diffractometer. The data were corrected for Lorentz and polarization effects as well as for the absorption. The structures of all compounds were solved by direct methods using (SIR97)^{23a} and refined on F^2 using least-squares refinement methods by SHELXL-97.^{23b} All non-hydrogen atoms were refined using anisotropic thermal parameters. The hydrogen atoms were included in ideal positions (unless specified) with a fixed U_{iso} value and were riding on their respective non-hydrogen atoms. The O5 and O6 in **L1** showed disorder, which could be resolved by splitting each of these atoms into two parts with their site occupancy factors and thermal parameters refined as free variables. The hydrogens of the water molecules in **(1)** and **(1a)** were located from difference Fourier and were refined with their U_{iso} values 1.2 times that of the carrier oxygens and fixed O–H distance of 0.82(2) Å. Similarly the amide hydrogens in **L**, **L1**, **(1)**, and **(1a)** were located from difference Fourier and were refined with their U_{iso} values 1.2 times that of the carrier nitrogen atoms with fixed distance of 0.88(2) Å. The data measurement and other refinement parameters for these five crystal structures are given in Supporting Information, Table S1.

RESULTS AND DISCUSSION

Infrared Spectroscopy. **L** shows the $\nu_{\text{N-H}}$ band at 3272 cm^{-1} , strong amide I band at 1699 cm^{-1} , and $\nu_{\text{C-N}}$ at 1299 cm^{-1} (Figure S1, Supporting Information). The corresponding bands in **L1** are found at 3438, 1696, and 1300 cm^{-1} , respectively. The bands due to $\nu_{\text{OSO(asy)}}$ and $\nu_{\text{OSO(sym)}}$ appear at 1215 and 1012 cm^{-1} (Figure S2, Supporting Information). Complex **(1)** shows amide I band at 1631 cm^{-1} and $\nu_{\text{C-N}}$ at 1359 cm^{-1} , which are shifted from **L** indicating the coordination to copper through carbonyl oxygen and pyridine N atom (Figure S3, Supporting Information). Additional bands due to $\nu_{\text{OSO(asy)}}$ and $\nu_{\text{OSO(sym)}}$ appear in **(1)** at 1219 and 1015 cm^{-1} , and the $\nu_{\text{O-H}}$ band at 3424 cm^{-1} is indicative of the presence of coordinated and the noncoordinated water molecules. Complex **(2)** shows amide I bands at 1691 and $\nu_{\text{C-N}}$ 1309 cm^{-1} (Figure S4, Supporting Information) with a very slight shift in the former indicating no coordination through the amide group but only through the pyridine nitrogen. The presence of –OH and –NH bands at 3436 and 3271 cm^{-1} indicate water and amide hydrogen. Complex **(3)** shows $\nu_{\text{C=O}}$ amide I band at 1596 cm^{-1} and $\nu_{\text{C-N}}$ at 1304 cm^{-1} (Figure S5, Supporting Information) signifying that a deprotonated amide group^{6a,24} and pyridine are coordinating to the metal ion, respectively. The $\nu_{\text{S=O}}$ bands are conspicuous by their absence, both in **(2)** and **(3)** ruling out any oxidation.

UV-vis Spectroscopy. The absorption spectrum of complex **1** was measured both in the solid state and as well as in DMSO. The solid-state diffuse reflectance spectrum of **1** displays a broad absorption band at ca. 700 nm suggestive of a predominantly tetragonal geometry, in conformity with the X-ray structural result. In DMSO solution, complex **1** displays a band at 697 nm ($14\,347 \text{ cm}^{-1}$, $\epsilon = 57.4 \text{ M}^{-1} \text{ cm}^{-1}$), which has been assigned to $E_g \rightarrow T_{2g}$ d–d transition (Figure 1); the broadness is attributed to tetragonal distortion due to Jahn–Teller effect.²⁵ Another band at 290 nm ($34\,482 \text{ cm}^{-1}$, $\epsilon = 23\,540 \text{ M}^{-1} \text{ cm}^{-1}$) was assigned tentatively to a charge transfer (CT) transition. The extinction coefficient values justify the assignment of the transitions. Importantly, the DMSO solution

absorption spectrum is in complete similarity to that of solid-state spectrum. This strongly suggests that the solid-state tetragonal geometry around the Cu(II) ion is maintained in the DMSO solution. However, it is likely that the coordinated water molecules may dissociate in solution and be replaced by the solvent molecules.

The absorption spectrum of complex **3** was measured both in the solid state and in two solvents of different polarity (DMSO and MeOH, Figure 1). The diffuse reflectance spectrum of **3** displays a broad spectral feature centered on 800 nm in addition to ill-defined features at ca. 500 and ca. 400 nm. As the crystal structure of this complex exhibits the presence of both four- as well as five-coordinate cupric ions, the solid-state absorption spectrum appears to be a bit complex. Interestingly, the solution-state absorption spectrum is quite different from that of the solid-state one implying that in going from solid to the solution phase, a stereochemical change around Cu(II) ion has occurred. In fact, it is likely that the tetranuclear structure breaks in solution generating two dinuclear molecules. In particular, MeOH solution displays transitions at 736 nm ($13\,586 \text{ cm}^{-1}$) with low extinction coefficient of $48.6 \text{ M}^{-1} \text{ cm}^{-1}$ and a high-energy feature at 302 nm ($33\,112 \text{ cm}^{-1}$, $\epsilon = 10\,570 \text{ M}^{-1} \text{ cm}^{-1}$). The DMSO solution, on the other hand, shows transitions at 911 nm ($10\,976 \text{ cm}^{-1}$, $\epsilon = 96 \text{ M}^{-1} \text{ cm}^{-1}$) and 374 nm ($26\,737 \text{ cm}^{-1}$, $\epsilon = 1874 \text{ M}^{-1} \text{ cm}^{-1}$). In both solvents, the low-energy feature can be assigned to d–d transition considering its position and low extinction coefficient, whereas the high-energy feature is tentatively assigned to ligand-to-metal CT band. The presence of both thiolate and thioether functional groups in complex **3** suggests the possibility of CT.^{6a}

X-ray Crystal Structures. The X-ray crystal structure of **L** (Figure 2) shows that in two halves of the molecule (about S–S

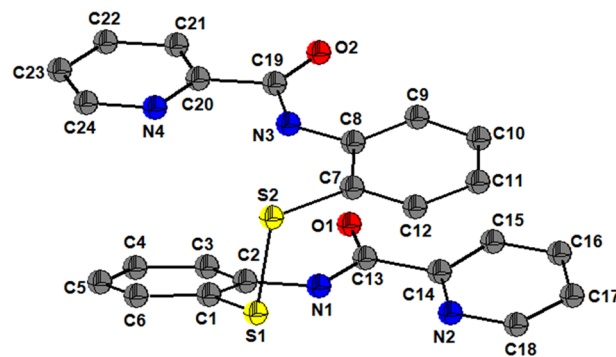


Figure 2. ORTEP view of the final model of disulfide compound **L** at 50% probability.

bond) the pyridine and the phenyl ring are forming very different dihedral angles ($24.9(1)$; $8.7(1)^\circ$) between them, signifying that one-half is relatively more planar than the other. Similarly the dihedral angles between the two pyridine rings and two phenyl rings are rather unequal [$7.5(1)$ and $26.3(1)^\circ$]. The torsion angle C12-S1-S2-C24 is 89.1° in the molecular structure of **L** and shows a kink around the S–S bond making the two halves out of plane with each other. The conformation adopted gives $\pi \cdots \pi$ interactions between the pyridine ring (N1, C1–C5) and phenyl ring (C19–C24) with *centroid to centroid* distance as 3.89 Å, whereas the same between the other pair is longer (4.12 Å) (Figure S6, Supporting Information).

The sulfinato ligand **L1** (Figure 3) has four disordered oxygens. Compared to **L**, the torsion angle C12-S1-S2-C24

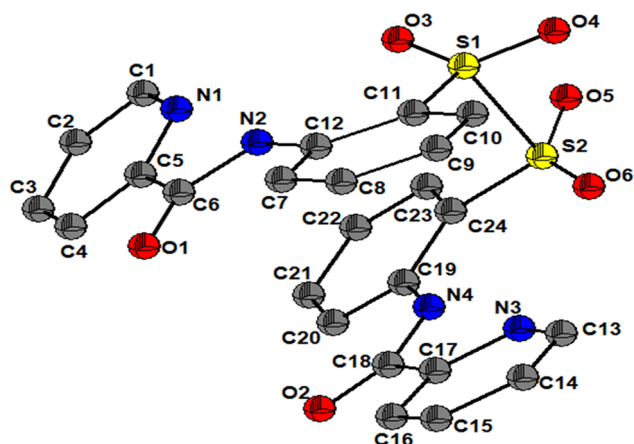


Figure 3. ORTEP view of the final model of sulfinato compound **L1** at 50% probability.

is slightly decreased to 82.8° . In each half of the molecule, the dihedral angles between pyridine and the phenyl ring are $29.8(1)$ and $17.3(1)^\circ$, which are close to each other, showing that now both halves are significantly nonplanar. Similarly the two pyridine rings and the two phenyl rings are making dihedral angles of $19.5(2)$ and $27.6(1)^\circ$, which are again relatively close to each other compared to those found in **L**. The orientation gives face-to-face $\pi\cdots\pi$ interactions between the pyridine ring of one half and the phenyl ring of the other half (centroid to centroid distance 3.3 and 3.9 Å, Figure S7, Supporting Information). The amide nitrogens N2 and N4 are intramolecularly H-bonded to pyridine nitrogens N1 and N3 and sulfinate oxygens O3 and O6, respectively. (Figure 3, Table S2, Supporting Information).

In (**1**), the centrosymmetric Cu(II) ion has an octahedral environment (Figure 4) from two water molecules and two

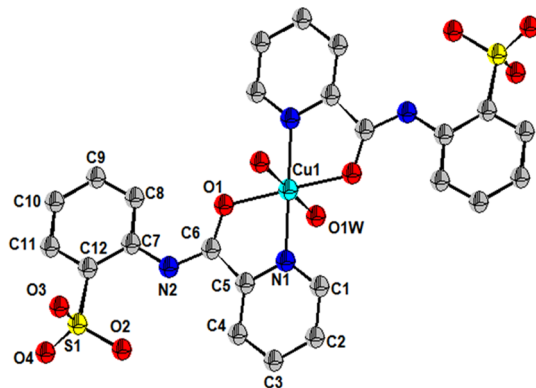


Figure 4. ORTEP view of complex (**1**); hydrogen atoms were removed for clarity (50% probability).

bidentate **L2** ligand molecules, bonding through pyridine and carbonyl oxygen. The charge neutrality in the complex is maintained by the two sulfonate (SO_3^-) units. Cu1–N1 and Cu1–O1 distances are 1.967(8) Å and 1.998(7) Å, respectively, whereas the Cu1–O1W distance 2.373(11) Å is rather long showing the well-known Jahn–Teller distortion. The S1–O3 and S1–O4 distances are equal to 1.439(2) Å, whereas the S1–O2 distance 1.448(2) Å is slightly longer as it is forming strong intramolecular H-bonds with amide N2 (Table S2, Supporting Information), which is also H-bonded with S1. The remaining two sulfonate oxygens are engaged in strong intermolecular H-

bonding interactions with water molecule O1W, forming a 2D H-bonded network running diagonally parallel to the *ab* plane (Figure 5). This 2D structure consists of 12-membered rings of H-bonded water and sulfonate groups, which are further joined to each other through coordination of metal ions.

The ligand **L** when treated with $\text{Cu}(\text{ClO}_4)_4 \cdot 6\text{H}_2\text{O}$ gives the same crystal structure with same space group but when treated with $\text{Cu}(\text{NO}_3)_2$ in same reaction conditions forms complex (**1**), which crystallizes in monoclinic $P2_1/n$ space group, and thus is a polymorph of (**1**), being referred to as (**1a**) henceforth. The geometry around the central metal ion is the same as in (**1**). The bond lengths of Cu1–N1 and Cu1–O1 of 2.006(3) and 2.294(3) Å, respectively, found in (**1a**) are longer than those found in (**1**), whereas the Cu1–O1W distance in (**1a**) is shorter (1.9732(3) Å) than the corresponding distance in (**1**) (2.373(10) Å). These bond distances clearly show that Cu(II) ion in (**1**) has a “z out” tetragonal distortion, whereas it is having a “z in” tetragonal distortion in (**1a**) (Figure 6). The bond angles N1–Cu1–O1 are $82.03(3)$ and $75.59(9)^\circ$ in (**1**) and (**1a**), respectively, showing that the bite angle of the ligand is smaller in the latter. The dihedral angle between the coordination planes passing through N1, O1, Cu1, N1', O1', and the phenyl ring (C7 to C12) is $15.15(4)^\circ$ in (**1**) and $12.97(9)^\circ$ in (**1a**) further supporting that the molecule has different conformations in the two crystal forms. The S–O bond distances in (**1a**) are in the range from 1.383(4) to 1.392(5) Å, which are shorter than those found in (**1**). It may be due to the unresolved disorder in the sulfonate group in (**1a**).

As in (**1**), one of the sulfonate oxygens, namely, O3 is forming intramolecular H-bond with the amide N2, which is also donating a H-bond to S1 (Supporting Information, Table S2). Similarly the remaining two oxygens O2 and O4 are involved in strong intermolecular H-bonding interactions with water molecules. The packing consists of undulating chains—formed of water molecules and the sulfonate groups only—which are further arranged in an antiparallel arrangement running diagonally parallel to the *ac* plane, due to the coordination of water to metal ions (Figure 7). The water \cdots sulfonate intermolecular H-bonding distances are shorter in (**1a**) (Supporting Information, Table S2) indicating a relatively strong H-bonding.

Complex (**3**) is a tetranuclear centrosymmetric complex (Figure 8) that is formed by chloride bridging between two dinuclear units, with two Cu(II) ions in different stereochemistry. In each unit Cu1 is five-coordinated by one pyridine N1, one deprotonated amide nitrogen N2, one thioether sulfur S2, one bridging thiol S1, and one bridging chloride ion Cl1, whereas Cu2 is four-coordinated by pyridine N3, amide nitrogen N4, bridging thiol S2, and Cl1. Cu1 is in a square pyramidal geometry with chloride in the axial position and Cu1 above the plane (0.36 Å) of the four equatorial donors, while Cu2 is nearly in a square plane (lying 0.1 Å above the plane). The tetranuclear complex has alternating, corner sharing of square planes with square pyramidal polyhedra (Figure 8, inset). Both chloride and thiol S1 show unsymmetrical bridging (Table S3, Supporting Information) between two polyhedra with relatively shorter bonds to the four-coordinated Cu2 ion. The two halves of the carboxamide unit in **L3** are almost perpendicular to each other (dihedral angle $75.89(4)^\circ$), and consequently the two coordination polyhedra are also forming a dihedral angle of $62.4(1)^\circ$ between them. Thus, the tetranuclear moiety consists of two centrosymmetric L-shaped

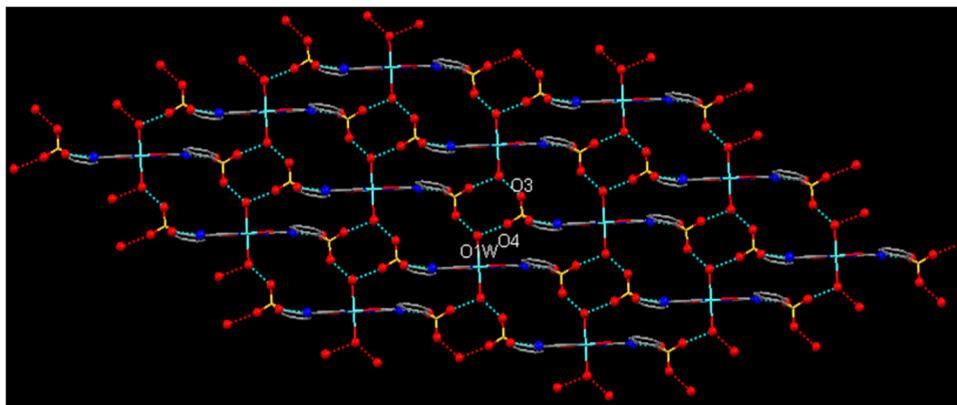


Figure 5. Crystal packing diagram of (1) showing 2D network due to H-bonding interactions.

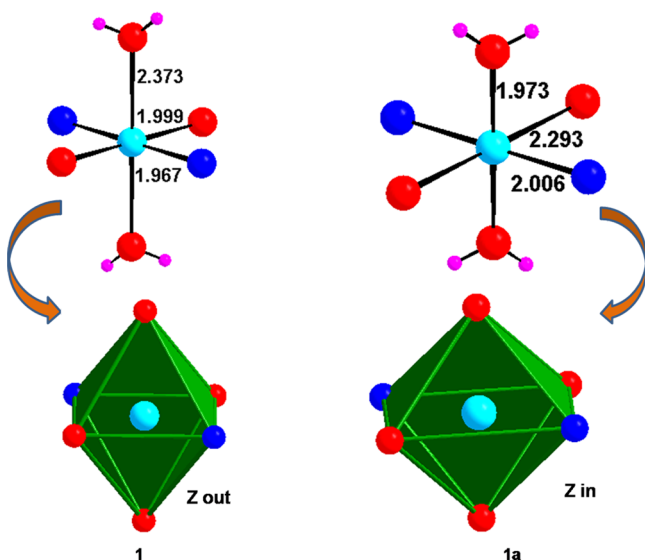


Figure 6. Showing z out and z in tetragonal distortions in (1) and (1a) crystalline forms.

dinuclear units bridged by the Cl^- ions. In the crystal structure of (3) these tetranuclear units are weakly H-bonded to each other (Table S2, Supporting Information) and also have $\pi\cdots\pi$ interactions between pyridine and phenyl rings to build a 2D H-bonded network in the (001) plane (Figure 9).

Cyclic Voltammetric Studies. The electrochemical behavior of complexes 1 and 3 was studied by CV at platinum working electrode. In DMSO solution, both complexes exhibit two reductive responses; first for the $\text{Cu}^{2+}/\text{Cu}^+$ couple (E_1) and the second one for the Cu^+/Cu^0 couple (E_2). The most cathodic response (E_2) was assigned to a Cu^+/Cu^0 process, since an anodic scan following an initial cathodic scan is associated with a sharp feature characteristic of desorption of electrochemically generated $\text{Cu}(0)$ species (Supporting Information, Figure S8).

The electrochemical behavior of complex 1 is displayed in Figure 10a, which represents two quasi-reversible reductive responses with E_1 value of 0.28 V versus SCE ($\Delta E_p = 250$ mV) and E_2 value of -0.44 V versus SCE ($\Delta E_p = 225$ mV). The observation of large ΔE_p (peak-to-peak separation = 220–250 mV) suggests a significant structural change during the course of electron transfer, which is expected given the different stereochemical preference for the $\text{Cu}(\text{II})$, $\text{Cu}(\text{I})$, and $\text{Cu}(0)$ states.²⁶ In addition, the $\text{Cu}(\text{II})$ ion in complex 1 is ligated to two water molecules, which are expected to be labile after the reduction thus contributing to the large ΔE_p values. The E_1 value for complex 1 was observed to be fairly positive suggesting a facile distortion of tetragonal geometry toward a tetrahedral one upon reduction to $\text{Cu}(\text{I})$ state. This is not unexpected considering the fact that the $\text{Cu}(\text{II})$ center is coordinated to two chelating ligands and therefore provides enough flexibility toward tetrahedral geometry.

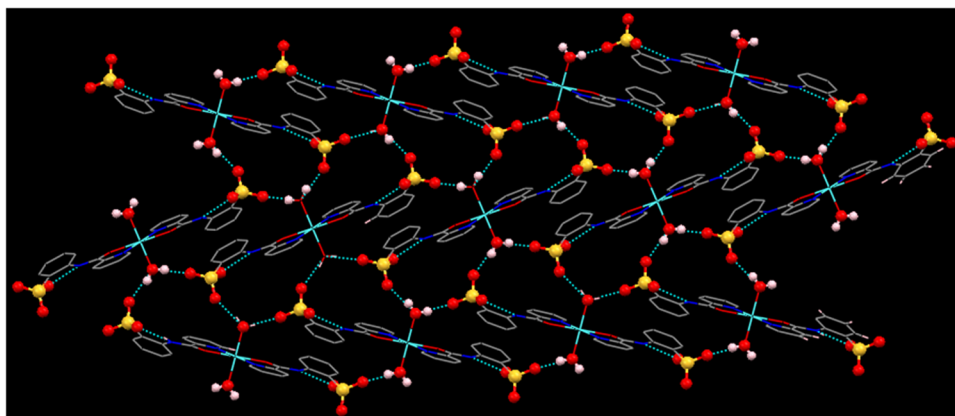


Figure 7. Crystal packing diagram of (1a) showing undulating chains of H-bonded water and sulfonates and the formation of 2D network by their antiparallel arrangement via coordination bonds.

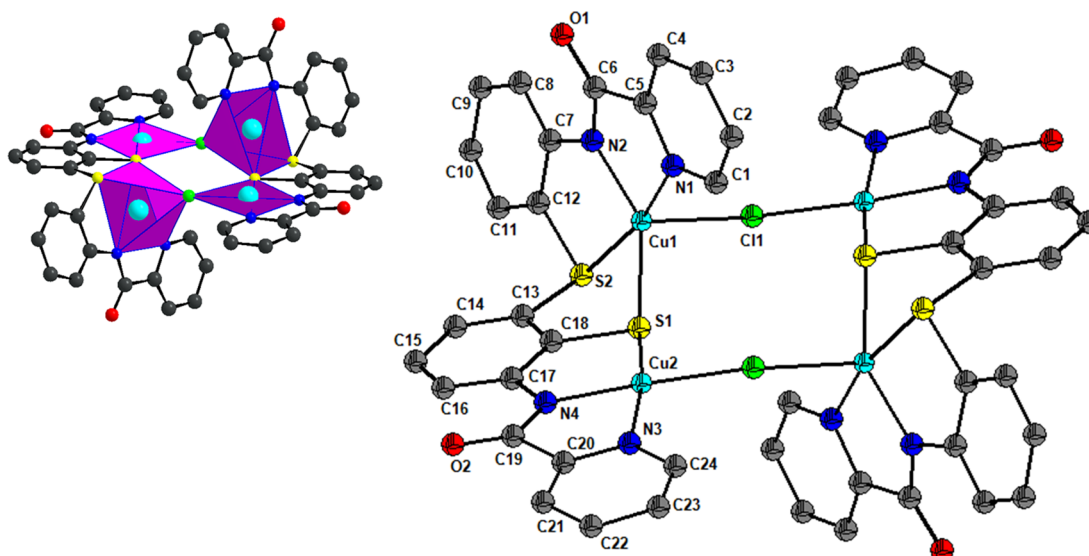


Figure 8. ORTEP view of complex (3) at 50% probability; hydrogen atoms were removed for clarity. (inset) Alternating corner sharing of square planes with square pyramidal polyhedra.

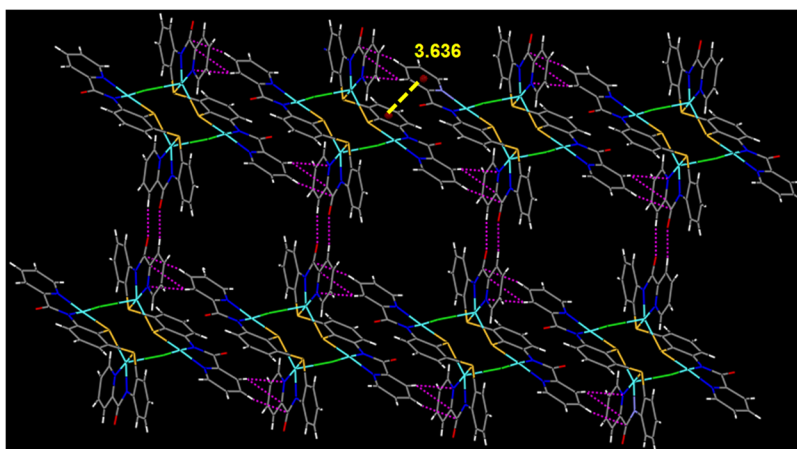


Figure 9. Crystal packing diagram of (3) showing C–H...O H-bonding and π ... π interactions to build 2D H-bonded network.

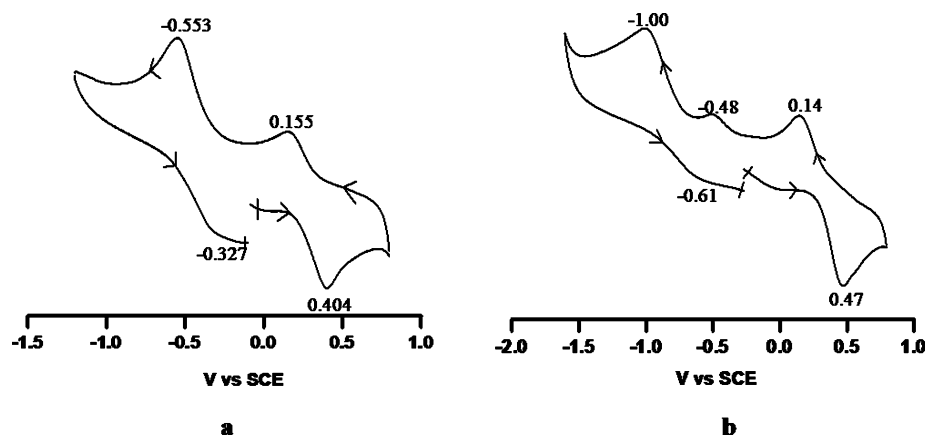


Figure 10. (a) CV of complex 1 displaying $\text{Cu}^{2+}/\text{Cu}^+$ (E_1) and Cu^+/Cu^0 (E_2) couples in DMSO at Pt working electrode; Pt wire as the counter electrode; and Ag/Ag^+ as the reference electrode. The potentials were corrected and reported vs SCE. (b) CV of complex 3 displaying $\text{Cu}^{2+}/\text{Cu}^+$ (E_1) and Cu^+/Cu^0 (E_2) couples in DMSO. The response at -0.48 V is due to some electrochemically generated Cu(I) species.

The electrochemical responses for complex 3 (Figure 10b) were of a very similar nature to that of complex 1, however, with sizable potential difference, particularly for the E_2

response. For this complex, the E_1 response was observed at 0.31 V with ΔE_p value of 330 mV. This response was assigned to $\text{Cu}^{2+}/\text{Cu}^+$ couple, however, with a much larger structural

change. We believe that the involvement of deprotonated N_{amidate} and S_{thiolate} in the coordination sphere must have significantly disfavored the tetrahedral geometry after reduction to Cu(I) state. Such a postulation is strengthened by the observation of Cu^+/Cu^0 process at a considerably lower potential of -0.81 V versus SCE ($\Delta E_p = 390$ mV) when compared to -0.44 V noted for complex **1**. This comparison suggests that the copper centers in complex **3** are coordinated to electron-rich donor groups, thus stabilizing the Cu(II) state to a large extent.

Thermogravimetric Analysis. Complex (**1**) (Figure 11) first shows loss of two and a half lattice water molecules, at 100

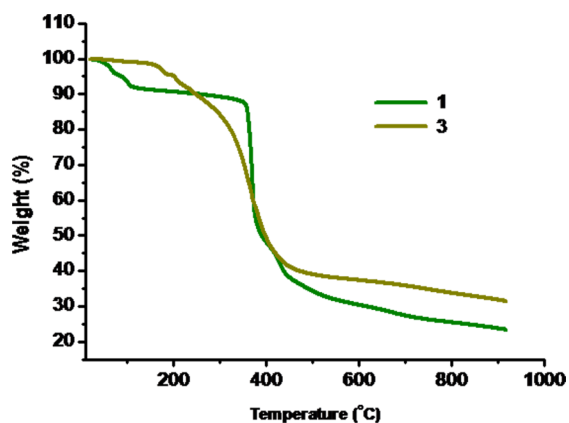


Figure 11. Thermogravimetric plot of the complexes (**1**) and (**3**).

°C (expected weight loss = 6.4% and observed weight loss = 6.6%). Subsequent decomposition occurs only after 350 °C when the organic part is lost in three consecutive steps; from 352 to 374, 400–500, and 500–900 °C, leaving a residue of Cu_2S , accounting for an observed residual weight of 23.33% against the calculated 23.34%. The high thermal stability of the complex is attributed to the 2D extended strong H-bonded network of the compound. A high weight loss rate and the

sharp thermal decomposition threshold are the features desirable for the compounds, which could be used as optical recording materials.²⁷

Complex (**3**) (Figure 11) shows first the weight loss of chlorine (expected weight loss = 5.70% and observed weight loss = 5.20%) at 200 °C. The loss of the organic ligand occurs in two steps in the range of 210–900 °C with 63.48% weight loss (observed weight loss = 63.68%). Finally above 916 °C, CuS was left as final residue (expected weight loss = 30.9% and observed weight loss = 31.4%).

NMR Spectroscopy. As (**2**) is insoluble in any solvent, its spectrum was taken in TFA + $CDCl_3$. The intensity ratio of protons in 1H NMR of **L** in TFA + $CDCl_3$ shows (Figure S14, Supporting Information) that two phenyl rings have become inequivalent and shift downfield (δ 7.03 to 7.79 and 8.06 to 8.22 ppm), and all the eight pyridine protons appear as a broad signal at δ 8.72, whereas the amide protons appear much downfield shifted at δ 10.46 ppm. That may be due to the interaction of pyridine and amide nitrogens with TFA making the two halves chemically inequivalent. The formation of complex (**2**) is indicated (Figure 12) by the restoration of the eight separate signals of **L**, with the phenyl protons shifted upfield relative to **L** (δ 7.26 to 7.72), the H_h and H_e protons of pyridine lying much downfield shifted at δ 8.81 and 9.01 ppm, respectively, and amide signal at δ 9.9 ppm. The changes in NMR indicate binding of Ag^+ ion with the pyridine nitrogens. The chemical analysis, including the molecular ion peak in the HRMS spectrum (Figure S18, Supporting Information) for (**2**) at the m/z value of 663.4305 for $[(AgL(NO_3)(H_2O)_2 - 1)^+]$ ion (calculated 663.4585) and the IR spectrum, corroborates the characterization of (**2**) as a complex of Ag^+ with the uncleaved disulfide ligand **L**.

Cleavage of S–S Bond. The two main reactions of thiol–disulfide systems—cleavage of the disulfide bond and oxidation of thiol to disulfide—were observed for **L** in the presence of Cu(II) ions. Disulfide bond is known to be broken by metal ions,^{28–31} but the mechanism of S–S bond cleavage is quite complicated and may follow many pathways.¹⁵ In the metal-

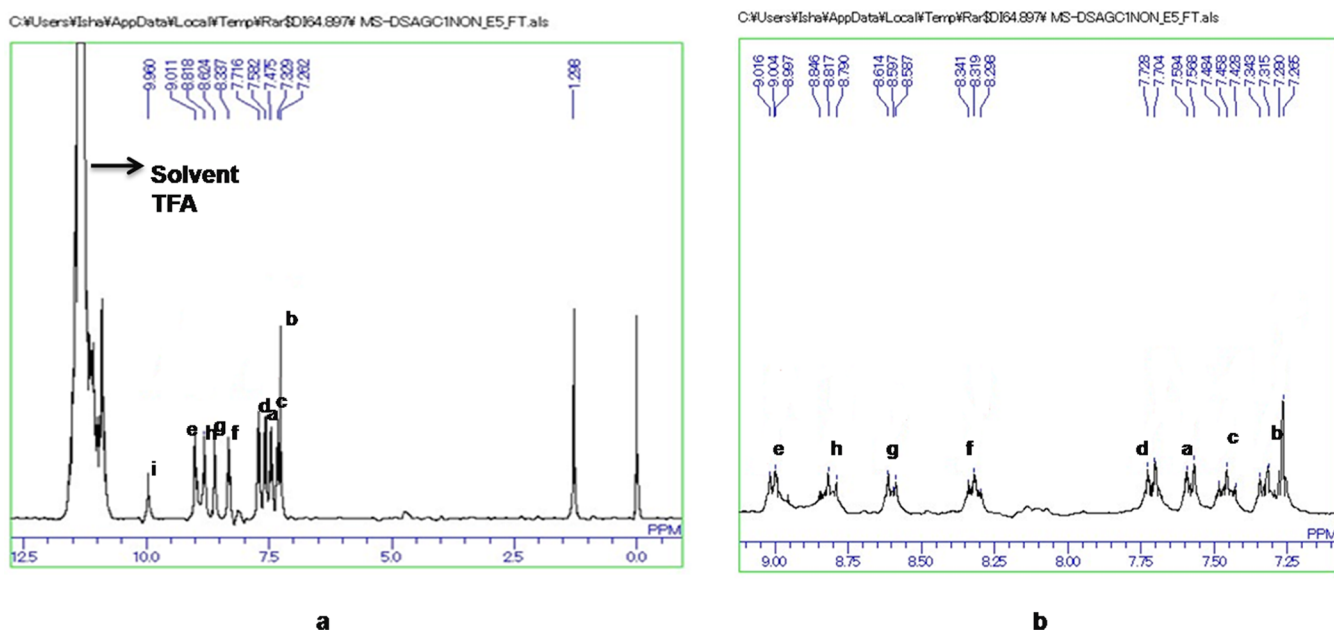


Figure 12. (a) The 1H NMR of complex (**2**) in TFA + $CDCl_3$ and (b) the expanded aromatic region.

assisted S–S cleavage, in water the mechanism is considered to involve an initial electrophilic attack by the metal ions on the S–S bond. Subsequent attack by the nucleophile (H₂O) results in a homolytic cleavage into RSH and RSOH. The formation of sulfinate complex follows the disproportionation of the unstable R–SOH with water in the presence of oxygen.²⁹ The thiol formed reduces Cu(II) to Cu(I), and some disulfide is reformed. The reaction products and their yields are found to be dependent on synthetic conditions like solvent, counterions, aerobic/anaerobic environment, and metal ions.²⁹ The S–S bond cleavage in bis(2-pyridylthio)methane was seen only with copper(II), and Co(II) and Ni(II) did not give any cleavage products, signifying the necessity of Cu(II)/Cu(I) redox couple. In the present case, Cu(II) gives a higher oxidized product, available after oxidative cleavage only, whereas Ag(I) did not cleave the bond and gave sulfinate only in a very small yield with a large amount of unreacted L or its (uncharacterized) Ag(I) complex. It may be because Cu(II), with higher charge/radius ratio, is more electrophilic than Ag(I) and polarizes the S–S bond to a greater extent.

In our system, all four kinds of products, that is, disulfide → thiolate → sulfinate → sulfonate were observed, albeit under different reaction conditions. The formation of thiolate, which gave (3), was observed in the presence of copper(II) chloride under anaerobic conditions in dry acetonitrile. The product was crystallized in methanol in the presence of insufficient oxygen. However, if the crystallization is kept in open the colorless disulfide L crystallizes, which was confirmed by its crystal structure. It is in concurrence with the reduction of Cu(II) by thiol and its own oxidation back to disulfide (L) (*vide supra*). L is always found to coexist with other products in different amounts, even in the aerobic oxidation reactions. Thus, it confirms the homolytic cleavage of the S–S bond as one of the steps in oxidation. Lago et al.²⁹ studied the effect of counteranion on the oxidized product of 2,2'-dipyridyldisulfide (dpds) and observed that weakly coordinating anions guide such reactions toward more oxidized species. In our case also, the reactions of L in aerobic conditions with copper(II) chloride, copper(II) perchlorate, and copper(II) nitrate gave sulfonates, thus endorsing their findings. Copper(II) chloride, however, under anaerobic conditions gives thiol, which when left with protic solvent methanol, in the presence of oxygen, oxidizes back to disulfide. Similarly the formation of sulfonate was observed in THF/water system corroborating the earlier observation of the role of protic solvents in Cu(II)-catalyzed S–S cleavage.³⁰

CONCLUSION

In summary, we give a first report of both copper-catalyzed oxidative and reductive scissions of the S–S bond of L. The anion-assisted, oxidative cleavage in water, is complete and reproducible with Cu(II) up to sulfonates but not with Ag(I), which gives sulfinate, signifying the crucial role of copper(II) salts. The reductive cleavage gives thiols, which undergo a unique rearrangement to form L3, following a C–S bond formation. The results are relevant for designing the reaction conditions to obtain a desired product and generate *in situ* ligands not easily accessible otherwise. Though the complete mechanism cannot be commented upon, the results here support the well-accepted view that the S–S cleavage is facilitated by concomitant electrophilic and nucleophilic attack by the metal ion and water/protic solvent, respectively.³² The reaction scheme followed here covers a complete cycle starting

from auto oxidation of thiol to disulfide and then reduction of disulfide to thiol on one hand or oxidation of thiol to sulfinate and sulfonates on the other.

ASSOCIATED CONTENT

Supporting Information

Spectral data, PXRD, crystal structure data, structural diagrams, and CCDC details. This material is available free of charge via the Internet at <http://pubs.acs.org>.

AUTHOR INFORMATION

Corresponding Authors

*E-mail: hundal_chem@yahoo.com.

*E-mail: geetahundal@yahoo.com. Fax: +91 0183 2258820. Phone: +91 9501114468.

Notes

The authors declare no competing financial interest.

ACKNOWLEDGMENTS

G.H. is thankful to Council of Scientific and Industrial Research, India for financial support, I.L. is thankful to University Grants Commission for fellowship. We gratefully acknowledge the help rendered to us by Dr. R. Gupta, Department of Chemistry, Delhi University, Delhi for CV measurements and interpretation and also to Dr. K. R. J. Thomas, Department of Chemistry, IIT Roorkee, for the TGA measurements.

REFERENCES

- (1) (a) Swaisgood, H. E. *Biotechnol. Adv.* **2005**, *23*, 71. (b) Gupta, A.; Van Vlijmen, H. W. T.; Singh, J. *Protein Sci.* **2004**, *13*, 2045. (c) Meinhold, D.; Beach, M.; Shao, Y.; Osuna, R.; Colon, W. *Biochemistry* **2006**, *45*, 9767.
- (2) (a) Gilbert, B. C.; Silvester, S.; Walton, P. H.; Whitwood, A. C. *J. Chem. Soc., Perkin Trans.* **1999**, *2*, 1891. (b) Jacob, C.; Giles, G. L.; Giles, N. M.; Sies, H. *Angew. Chem., Int. Ed.* **2003**, *42*, 4742.
- (3) (a) Humphrey, S. M.; Mole, R. A.; Rawson, J. M.; Wood, P. T. *Dalton Trans.* **2004**, 1670. (b) Caradoc-Davies, P. L.; Hanton, L. R. *Dalton Trans.* **2003**, 1754. (c) Horikoshi, R.; Mochida, T.; Moriyama, H. *Inorg. Chem.* **2002**, *41*, 3017. (d) Huang, Ch.; Gou, S.; Zhu, H.; Huang, W. *Inorg. Chem.* **2007**, *46*, 5537.
- (4) (a) Thompson, A. M. W. C.; Bardwell, D. A.; Jeffery, J. C.; Rees, L. H.; Ward, M. D. *J. Chem. Soc., Dalton Trans.* **1997**, 721. (b) Thompson, A. M. W. C.; Blandford, I.; Redfearn, H.; Jeffery, J. C.; Ward, M. D. *J. Chem. Soc., Dalton Trans.* **1997**, 2661. (c) Shinkai, S.; Inuzuka, K.; Miyazaki, O.; Manabe, O. *J. Am. Chem. Soc.* **1985**, *107*, 3950.
- (5) (a) Murata, M.; Kojima, M.; Hiokia, A.; Miyagawa, M.; Hirotsu, M.; Nakajima, K.; Kita, M.; Kashino, S.; Yoshikawa, Y. *Coord. Chem. Rev.* **1998**, *174*, 109. (b) Henderson, R. K.; Bouwman, E.; Spek, A. L.; Reedijk, J. *Inorg. Chem.* **1997**, *36*, 4616.
- (6) (a) Tyler, L. A.; Noveron, J. C.; Olmstead, M. M.; Mascharak, P. K. *Inorg. Chem.* **2000**, *39*, 357. (b) Wang, D.; Behrens, A.; Farahbakhsh, M.; Gatjens, J.; Rehder, D. *Chem.—Eur. J.* **2003**, *9*, 1805.
- (7) (a) Huang, Ch.; Gou, S.; Zhu, H.; Huang, W. *Inorg. Chem.* **2007**, *46*, 5537. (b) Han, L.; Bu, X.; Zhang, Q.; Feng, P. *Inorg. Chem.* **2006**, *45*, 5736. (c) Wang, J.; Zhang, Y.-H.; Li, H.-X.; Lin, Z.-J.; Tong, M. L. *Cryst. Growth Des.* **2007**, *7*, 2352. (d) Wang, J.; Zheng, S.-L.; Li, H.-X.; Hu, S.; Zhang, Y.; Tong, M. L. *Inorg. Chem.* **2007**, *46*, 795. (d) Delgado, S.; Gallego, A.; Castillo, O.; Zamora, F. *Dalton Trans.* **2011**, *40*, 847.
- (8) (a) Wang, Y.; Espenson, J. H. *J. Org. Chem.* **2000**, *65*, 104. (b) Khiar, N.; Mallouk, S.; Valdivia, V.; Bougrin, K.; Soufiaoui, M.; Fernandez, I. *Org. Lett.* **2007**, *9*, 1255. (c) Murray, R. W.; Jindal, S. L. *J. Org. Chem.* **1972**, *37*, 3516.

- (9) (a) Lowe, G. O. *J. Org. Chem.* **1976**, *41*, 2061. (b) Esparza-Ruiz, A.; Gonzalez-Gomez, G.; Mijangos, E.; Pena-Hueso, A.; Lopez-Sandoval, H.; Flores-Parra, A.; Contreras, R.; Barba-Behrens, N. *Dalton Trans.* **2010**, *39*, 6302.
- (10) (a) Scrivens, G.; Gilbert, B. C.; Lee, T. C. P. *J. Chem. Soc., Perkin Trans.* **1995**, *2*, 955. (b) Pispisa, B.; Paradossi, G.; Palleschi, A.; Desideri, A. *J. Phys. Chem.* **1988**, *92*, 3422. (c) Neyaglov, A. A.; Digurov, N. G.; Bukharkina, T. V.; Mazgurov, A. M.; Fakhriev, A. M. *Kinet. Catal.* **1991**, *32*, 479. (d) Wallace, T. J. *J. Org. Chem.* **1966**, *31*, 3071. (e) Nakaya, T.; Arabori, H.; Tmoto, M. *Bull. Chem. Soc. Jpn.* **1970**, *43*, 1880. (f) Wallace, T. J. *J. Org. Chem.* **1966**, *31*, 1217. (g) Papadopoulos, E. P.; Jarrar, A.; Issidorides, C. H. *J. Org. Chem.* **1966**, *31*, 615. (h) Coates, R. J.; Gilbert, B. C.; Lee, T. C. P. *J. Chem. Soc., Perkin Trans.* **1992**, *2*, 1387. (i) Mukaiyama, T.; Endo, T. *Bull. Chem. Soc. Jpn.* **1967**, *40*, 2388. (j) Capozzi, G.; Modena, G. Oxidation of Thiols. In *Chemistry of the Thiol Group*, Part 2; Patai, S., Ed.; Wiley: Hoboken, NJ, 1974; p 785. (k) Kalinina, E. I.; Lukina, E. M.; Masleunikov, V. P. *Tr. Khim. Khim. Tekhnol.* **1967**, *190*. (l) McKillop, A.; Koyungu, D.; Krief, A.; Dumont, W.; Renier, P.; Trabelsi, M. *Tetrahedron Lett.* **1990**, *31*, 5007. (m) Wallace, T. J.; Schriesheim, A. *J. Org. Chem.* **1962**, *27*, 1514. (n) Wallace, T. J.; Schriesheim, A. *Tetrahedron* **1965**, *21*, 2271. (o) Wallace, T. J.; Schriesheim, A.; Bartok, W. *J. Org. Chem.* **1963**, *23*, 1311.
- (11) Seko, H.; Tsuge, K.; Igashira-Kamiyama, A.; Kawamotob, T.; Konno, T. *Chem. Commun.* **2010**, *46*, 1962.
- (12) Bhattacharya, A. K.; Hortmann, A. G. *J. Org. Chem.* **1978**, *43*, 2728.
- (13) Wang, Y.; Espenson, J. H. *J. Org. Chem.* **2000**, *65*, 104.
- (14) (a) Oae, S. *Organic Sulfur Chemistry: Structure and Mechanism*; CRC Press: Boca Raton, FL, 1991; Vol. 1, pp 213–216. (b) Allen, P., Jr.; Brook, J. W. *J. Org. Chem.* **1962**, *27*, 1019.
- (15) Higashi, L. S.; Lundeen, M.; Hilti, E.; Seff, K. *Inorg. Chem.* **1977**, *16*, 311.
- (16) Kimura, K.; Kimura, T.; Kinoshita, I.; Nakashima, N.; Kitano, K.; Nishioka, T.; Isobe, K. *Chem. Commun.* **1999**, 497.
- (17) Delgado, S.; Molina-Ontoria, A.; Medina, M. E.; Pastor, C. J.; Jiménez-Aparicio, C. R.; Priego, J. L. *Inorg. Chem. Commun.* **2006**, *9*, 1289.
- (18) (a) Raper, E. S. *Coord. Chem. Rev.* **1994**, *129*, 91. (b) Oae, S.; Okuyama, T. *Organic Sulfur Chemistry: Biochemical Aspects*; CRC Press: Ann Arbor, MI, 1992; pp 1–43.
- (19) Carballo, R.; Covelo, B.; Fernandez-Hermida, N.; Lago, A. B.; Vazquez-Lopez, E. M. *CrystEngComm* **2009**, *11*, 817.
- (20) (a) Lumb, I.; Hundal, M. S.; Corbella, M.; Gomez, V.; Hundal, G. *Eur. J. Inorg. Chem.* **2013**, 4799. (b) Lumb, I.; Hundal, M. S.; Mathur, P.; Corbella, M.; Aliaga-Alcalde, N.; Hundal, G. *Polyhedron* **2012**, *36*, 85.
- (21) Armarego, W. L. F.; Perrin, D. D. *Purification of Laboratory Chemicals*, 4th ed; Butterworth-Heinemann: Oxford, U.K., 1996.
- (22) Shendage, M.; Frohlich, R.; Haufe, G. *Org. Lett.* **2004**, *6*, 3675.
- (23) (a) Altomare, A.; Burla, M. C.; Camalli, M.; Cascarano, G.; Giacovazzo, C.; Gualardi, A.; Moliterni, A. G. G.; Polidori, G.; Spagna, R. *J. Appl. Crystallogr.* **1999**, *32*, 115. (b) Sheldrick, G. M. *SHELX-97: Program for Refinement of Crystal Structures*; University of Göttingen: Göttingen, Germany, 1997.
- (24) Jubert, C.; Mohamadou, A.; Gerard, C.; Brandes, S.; Tabard, A.; Barbier, J.-P. *J. Chem. Soc., Dalton Trans.* **2002**, 2660.
- (25) Lever, A. B. P. *Inorganic Electronic Spectroscopy*, 1st ed.; Elsevier: Amsterdam, 1968; pp 355–357 and references 114, 266, and 319–321 mentioned therein.
- (26) (a) Kopylovich, M. N.; Nunes, A. C. C.; Mahmudov, K. T.; Haukka, M.; Leod, T. C. O. M.; Martins, L. M. D. R. S.; Kuznetsov, M. L.; Pombeiro, A. J. L. *Dalton Trans.* **2011**, *40*, 2822. (b) Zanello, P.; Vigato, P. A.; Mazzocchin, G. A. *Transition Met. Chem.* **1982**, *7*, 291. (c) Franco, E.; Torres, E. L.; Mendiolaand, M. A.; Sevilla, M. T. *Polyhedron* **2000**, *19*, 441. (d) Monzani, E.; uinti, L.; Perotti, A.; Casella, L.; Gulloti, M.; Randaccio, L.; Geremia, S.; Nardin, G.; Faleschini, P.; Tabbi, G. *Inorg. Chem.* **1998**, *37*, 553. (e) Monzon, L. M. A.; Burke, F.; Coey, J. M. D. *J. Phys. Chem. C* **2011**, *115*, 9182.
- (f) Ottenwaelder, X.; Aukauloo, A.; Journaux, Y.; Carrasco, R.; Cano, J.; Cervera, B.; Castro, I.; Curreli, S.; Munoz, M. C.; Rosello, A. L.; Soto, B.; Ruiz-Garcia, R. *Dalton Trans.* **2005**, 2516. (g) Carrasco, R.; Cano, J.; Ottenwaelder, X.; Aukauloo, A.; Journaux, Y.; Ruiz-Garcia, R. *Dalton Trans.* **2005**, 2527. (h) Sharma, S. K.; Hundal, G.; Gupta, R. *Eur. J. Inorg. Chem.* **2010**, 621. (i) Munjal, M.; Kumar, Sushil; Sharma, S. K.; Gupta, R. *Inorg. Chim. Acta* **2011**, *377*, 144. (j) Gupta, M.; Mathur, P.; Butcher, J. *Inorg. Chem.* **2001**, *40*, 878. (k) Sivagnanam, U.; Palaniandavar, M. *J. Chem. Soc., Dalton Trans.* **1994**, 2277. (l) Pal, S.; Poddar, S. N.; Gosh, S.; Mukherjee, G. *Polyhedron* **1995**, *14*, 3023.
- (27) (a) Chen, Z.; Huang, F.; Wu, Y.; Gu, D.; Gan, F. *Inorg. Chem. Commun.* **2006**, *9*, 21. (b) Huang, F.; Wu, Y.; Gu, D.; Gan, F. *Thin Solid Films* **2005**, 483, 251.
- (28) Delgado, S.; Santana, A.; Castillo, O.; Zamora, F. *Dalton Trans.* **2010**, *39*, 2280.
- (29) Lago, A. B.; Amoedo, A.; Carballo, R.; Martinez, E. J.; Vazquez-Lopez, E. M. *Dalton Trans.* **2010**, *39*, 10076.
- (30) Zhu, H.-B.; Li, L.; Xu, G.; Gou, S.-H. *Eur. J. Inorg. Chem.* **2010**, 1143.
- (31) Delgado, S.; Barrilero, A.; Molina-Ontoria, A.; Medina, M. E.; Pastor, C. J.; Jimenez-Aparicio, R.; Priego, J. L. *Eur. J. Inorg. Chem.* **2006**, 2746.
- (32) Kice, J. L. *Acc. Chem. Res.* **1968**, *1*, 58.